Phase-Field Simulations of Crystal Growth

Mathis Plapp

Physique de la Matière Condensée, Ecole Polytechnique, CNRS, 91128 Palaiseau, France

Abstract. This course gives an elementary introduction to the phase-field method and to its applications for the modeling of crystal growth. Two different interpretations of the phase-field variable are given and discussed. It can be seen as a physical order parameter that characterizes a phase transition, or as a smoothed indicator function that tracks domain boundaries. Elementary phase-field models for solidification and epitaxial growth are presented and are applied to the dendritic growth of a pure substance and the step-flow growth on a vicinal surface.

Keywords: numerical simulations, phase-field models, solidification, epitaxial growth
PACS: 05.70.Ln, 64.70.Dv, 81.30.Fb

INTRODUCTION

The phase-field method had become during the last few decades a versatile and popular tool for numerical simulations of crystal growth and, more generally, for a multitude of moving boundary problems. Its main strong point is its algorithmic simplicity: the mathematical model amounts to a set of coupled differential equations that can be simulated using standard numerical techniques. Nevertheless, this method can easily deal with complex time-dependent geometries due to the representation of interfaces and boundaries by continuous fields, the so-called phase fields. They are almost constant within the domains occupied by different phases, and vary rapidly through well-localized but diffuse interfaces. Therefore, the phase-field model is a member of the larger family of *diffuse-interface models*. The history of such models can be traced back to van der Waals' treatment of the liquid-vapor interface [1] and Gibbs' work on the thermodynamics of diffuse interfaces [2]. In modern times, the steady increase in computational resources has led to the rapid development of more and more complicated models in such diverse fields as hydrodynamics [3], solidification [4,5,6,7,8], or solid-state phase transformations [9,10].

In the field of crystal growth, phase-field simulations have been mainly applied to two processes: solidification (an area that was instrumental for the development of the method, and in which the name "phase field" was actually coined) and epitaxial growth. On both topics, extensive recent reviews are available [4,5,6,7,8], and for solidification a relatively detailed pedagogical text can be found in Ref. [11]. The present short course is limited to an elementary introduction to the principles of the method and to some selected applications, and thus is not intended to give a complete picture of the field. Where appropriate, suggestions for further reading will be indicated.

The remainder of this article is organized as follows. In the next section, I will discuss two different ways of how to define the phase field, and how they can be advantageously combined to build simple but efficient models. Then, some applications of the model to solidification and to epitaxial growth will be described, followed by a brief conclusion.

WHAT IS THE PHASE FIELD ?

There are two complimentary ways to define the phase field. In the first, a coarse-graining procedure of a microscopic model leads to a continuum description on a larger length scale, whereas in the second, the smoothing of singularities leads to the appearance of a smaller length scale. Let us now examine each of these definitions in more details.

For a conceptual understanding of coarse-graining, it is useful to consider a simple two-phase system, for instance a fog, in which many small water droplets coexist with air that is saturated with water vapor. Furthermore, consider a simple averaged quantity such as the number density of water molecules. Its behavior depends on the scale on which the system is seen. More precisely, suppose that space is divided in an array of little cubes, and define the local number density as the number of water molecules present in a cube, divided by the volume of the cube. Here, the position of a molecule is defined by the position of its center of gravity, and a molecule is considered to be localized "in" a cube if its center of gravity is. If the cubes are of molecular size, they will contain zero or one molecule. In a water droplet, the probability to find one molecule in a cube is high, whereas in the vapor phase, the probability to find zero molecules is high. In both cases, the density changes rapidly with time for each cube by sudden jumps form zero to one molecule or back, which makes the density so defined quite useless for computations. For slightly larger cubes, there can be several molecules in a cube, and elementary statistical physics yields that for a cube occupied on average by N molecules, typical fluctuations are of the order $\sqrt{\mathbf{N}}$. Thus, the relative magnitude of the fluctuations decreases as the cube size increases. The idea of coarse-graining is to write, instead of the original microscopic equations of motion, an equation for the average density in each cube.

Of course, the evolution of the local average density depends also on other averaged quantities, such as energy, momentum, and entropy. For simplicity, let us assume that displacement of mass takes place by diffusion only, in which case the momentum equation can be discarded. If the size of the cubes is larger than the typical range of molecular interactions, the evolution of the density in one cube can only depend on the averaged quantities in the neighboring cubes. The resulting equations are universal and can be naturally derived form a free energy functional of Ginzburg-Landau type, which consists of a double-well potential and a gradient term. For a recent explicit calculation starting from a simple lattice-gas model, see [12]. An explicit example of a free energy functional will be given below. For now, let us just insist on two points: (i) all the coefficients of the free-energy functional depend a priori on the choice of the cube size, and (ii) obviously there is an upper cutoff on the allowed cube sizes. Indeed, in the above example of a fog, the interfaces between the water droplets and the vapor have a certain characteristic thickness (of the order of one nanometer). When the cube size becomes larger than this thickness, then the material inside the cube is no longer homogeneous, and the concept of a local average density has lost its meaning since the local value of the density will depend on which fraction of the cube is occupied by the water. The scale on which a system can be considered homogeneous is set by the correlation length, which can be much larger than the range of the molecular interactions when the system is close to a critical point.

Let us now take the opposite, macroscopic viewpoint. In this picture, interfaces are sharp surfaces (without a proper thickness), and the geometry of the two-phase system is described by the location of all the interfaces. The density now exhibits a jump from the inside to the outside of a droplet, and is mathematically described by a step function. Its evolution is governed by macroscopic laws which relate fluxes of extensive quantities (such as mass) to thermodynamic forces. A particular role is played by the surface tension, which gives rise to surface forces. For instance, consider a spherical droplet of radius R immersed in a vapor of fixed pressure. Laplace's law states that the pressure inside the droplet is higher than outside by an amount $2\gamma/R$, where γ is the surface tension. This is due to the compressive force which results from the surface tension, and which is localized at the interface. In mathematical terms, such a force is described by a Dirac delta function located at the surface, that is, the force density is infinite but acts on an infinitely fine surface, such that the total force (when integrated through the surface) remains finite.

This sharp-interface formulation can be perfectly used (and has been used) to perform numerical simulations. However, the handling of the interfaces (which must be discretized in some way) is cumbersome. An obvious idea to make this formulation more amenable to numerical treatment is to smooth out the singularities, that is, to replace step functions and surface delta functions by continuous profiles that have the shape of a smooth kink and a smooth peak, respectively. In this picture, the phase field is just the regularized step (or indicator) function. This regularization of singularities is a mathematically well-defined procedure, which introduces a new length scale into the problem, namely, the typical thickness W of the kink solution. Quite naturally, the resulting regularized problem will behave differently from the original singular problem, but the diffrerences disappear in the so-called *sharp-interface limit*, in which the thickness of the interface tends to zero while all the macroscopic scales remain fixed. A somewhat more sophisticated use of this procedure is the so-called *thin-interface limit*, in which the first-order corrections to the macroscopic problem are calculated and taken into account when choosing the parameters of the phase-field model. In that case, the first corrections to the sharp-interface problem scale as W^2, such that large values of W can be used. Such models have been termed *quantitative* in the literature [13,14,15]. Obviously, an upper limit for W is set by the other macroscopic scales present in problem. In the example given above, W must remain much smaller (in practice, about one order of magnitude) than the droplet size for the smoothened version of the problem to remain a correct description of the macroscopic geometry.

It is clear that, in the second approach, it is not necessary to start from a free energy functional. If the original sharp-interface equations are thermodynamically consistent, and the smoothing procedure is carried out correctly, the resulting phase-field model will faithfully reproduce the macroscopic dynamics. Indeed, an example for such a procedure is the phase-field model for Hele-Shaw flow developed in Ref. [16], which cannot be derived from a free energy functional but correctly describes the emergence of viscous fingers [17]. Thus, a free energy functional is *not* a necessary ingredient of a phase-field model. Nevertheless, models based on a free energy functionals remain the best starting point for the development of phase-field models, because they provide an immediate intuition about the model behavior, and because they permit to formulate models for new physical phenomena in a simple and straightforward way. However, it is important to stress that such models cannot be used for quantitative numerical simulations before a proper analysis of thin-interface effects has been carried out.

SOLIDIFICATION

Consider the solidification of a pure substance from its melt. In the following, we wish to describe the equiaxed dendritic growth of a single crystal from a homogeneously undercooled melt [18,19]. The difference in density between solid and liquid, generally small, is neglected, such that the growth of the crystal is limited only by the transport of heat. Furthermore, convection is neglected, such that the model consists of only two coupled equations: a diffusion equation for the heat, and the evolution equation for the phase field. The latter can be obtained from the free energy functional

$$F = \int \frac{K}{2}(\nabla\phi)^2 + Hf_{dw}(\phi) + \frac{L}{2T_m} g(\phi)(T - T_m), \tag{1}$$

where ϕ is the phase field, T the local temperature, T_m the melting temperature, L the latent heat of melting, and K and H are constants. Note that the interfacial anisotropy that is necessary to create dendrite arms has been neglected for simplicity; it will be discussed later on. The function $f_{dw}(\phi)$ is a double-well potential with minima for ϕ =1 (solid) and ϕ =-1 (liquid), and g(ϕ) is an interpolation function. Equation (1) has the typical form of a Ginzburg-Landau functional. The last two terms can be obtained by an expansion of the free energy density f(ϕ,T) of a homogeneous system around the melting point,

$$f(\phi,T) = f(\phi,T_m) + \left.\frac{\partial f(\phi,T_m)}{\partial T}\right|_{T_m} (T - T_m), \tag{2}$$

and by then rewriting the two terms of equation (2). At the melting point, the free energies of solid and liquid are the same, but the two phases are separated by a free energy barrier. Phenomenologically, this is captured by the double-well potential. Furthermore, the derivative of the free energy density is the negative of the entropy density, and the difference of entropy densities between the two phases, Δs, is related to the latent heat of melting by $L=T_m\Delta s$; taking into account that the difference between the two equilibrium values of the phase field is 2, equation (1) is obtained under the assumption that the interpolation function g(ϕ) satisfies g(1)=1 and g(-1)=-1.

Up to now, everything could have been obtained from a coarse-graining approach. Then, the phase field is the order parameter of the solid-liquid transition (for instance, a bond-angle order parameter as used in the interpretations of molecular dynamics simulations), and the coefficients K and H as well as the interpolation function g can be obtained from mean-field approximations. However, the resulting model would not be very useful for simulations. Indeed, the typical width of a solid-liquid interface is a few Angstroms, whereas a typical dendrite tip radius in of the order of microns, and the heat diffusion field surrounding the crystal is even much larger. In this situation, it is much more useful to switch to the view of the phase field as the smoothing of a macroscopic free boundary problem, and to *choose* appropriate values for the coefficients and functions.

To this end, a brief dimensional analysis is useful. Since F has the dimension of energy and the integral is over the volume, the coefficients K and H have units of energy/length and energy/volume, respectively. Thus, we can form two new quantities,

$$W = \sqrt{K/H} \qquad \gamma = I\sqrt{KH}\,, \tag{3}$$

with dimensions length and energy/surface, respectively. The first of these two is the typical thickness of the interface, and the second is the surface tension, where I is a numerical constant of order unity that depends on the choice of the double-well potential. Therefore, it is quite clear how to use this model in a phenomenological way:

since the capillary effect is a necessary physical ingredient, the value of γ needs to be correctly reproduced. In contrast, the interface thickness does not enter the problem in the macroscopic viewpoint, and can therefore be fixed at will. This can be achieved by choosing appropriate values for K and H.

Obviously, the above reasoning concerns only the equilibrium properties of the interfaces. A much more subtle question is how to achieve the correct interface kinetics. The complete answer can only be given by an asymptotic analysis of the dynamic model, which is out of the scope of the present contribution; details can be found in Ref. [13], and only the most important results will be stated here. To this end, let us non-dimensionalize the free energy functional and the temperature. The only non-trivial temperature scale present in the free solidification problem is the adiabatic temperature, L/c, where c is the specific heat (supposed to be identical for the two phases). The dimensionless temperature is then given by

$$u = \frac{T - T_m}{L/c}. \tag{4}$$

The free energy functional of equation (1) is divided by the constant H in order to obtain a dimensionless integrand,

$$\tilde{F} = \frac{F}{H} = \int \frac{W^2}{2}(\nabla\phi)^2 + f_{dw}(\phi) + \frac{IW}{2d_0} g(\phi) u, \tag{5}$$

where we have introduced the capillary length $d_0=\gamma c T_m/L^2$ and used the relations of equation (3). Note that, in this notation, it can be explicitly seen that the third term of the functional, which represents the thermodynamic driving force for interface motion, is proportional to the ratio W/d_0. The equation of motion for the phase field is then given by a functional derivative,

$$\tau\partial_t\phi = -\frac{\delta\tilde{F}}{\delta\phi} = W^2\nabla^2\phi - f'_{dw}(\phi) - \frac{IW}{2d_0} g'(\phi) u, \tag{6}$$

where τ is a relaxation time, to be determined below, and the primes denote derivation of the functions f_{dw} and g with respect to ϕ. For a homogeneous solid or liquid, the values of ϕ =1 and ϕ =-1, respectively, should be solutions of this equation, regardless of the temperature. This imposes that $g'(\pm 1) = 0$. It should be noted that, at this point, the interpretation of ϕ as an order parameter has to be abandoned. Indeed, any physical quantity (a bond-angle order parameter, for instance) will in general depend on the temperature. The advantage to choose ϕ as a smoothed indicator function becomes apparent when the equation for the temperature is written down. For the simplest case of equal thermal diffusivities D and in the two phases (symmetric model), it reads

$$\partial_t u = D\nabla^2 u + \frac{1}{2}\partial_t h(\phi), \tag{7}$$

where $h(\phi)$ is a function that satisfies h(1)=1 and h(-1)=-1. Since the phase field is almost constant outside of the interfaces, the source term on the right hand side is non-negligible only in the diffuse interfaces where the phase change takes place, and thus the function h simply describes the release or consumption of latent heat. For the choice $h(\phi)=g(\phi)$ the model is variational, that is, equations (6) and (7) can both be obtained from a single free energy functional [13]. However, for computational purposes, it is more advantageous to choose two different functions. In the following, we will specialize f_{dw}, g and h to be

$$f_{dw}(\phi) = -\frac{1}{2}\phi^2 + \frac{1}{4}\phi^4 \qquad g(\phi) = \frac{15}{8}\left(\phi - \frac{2}{3}\phi^3 + \frac{1}{5}\phi^5\right) \qquad h(\phi) = \phi. \tag{8}$$

For these choices, the equations of the model become

$$\tau\partial_t\phi = W^2\nabla^2\phi + \phi - \phi^3 - \lambda u\left(1-\phi^2\right)^2 \qquad \partial_t u = D\nabla^2 u + \frac{1}{2}\partial_t\phi, \tag{9}$$

where the dimensionless constant $\lambda=(15/16)IW/d_0$. It can be shown by asymptotic analysis [13] that, in the thin-interface limit, this phase-field model is equivalent to the macroscopic free boundary problem

$$\partial_t u = D\nabla^2 u, \tag{10}$$

$$v_n = \hat{n}\cdot\left(D\nabla u\big|_s - D\nabla u\big|_l\right), \tag{11}$$

$$u_{\text{int}} = -d_0\kappa - \beta v_n. \tag{12}$$

Here, the interface is sharp, $\hat{n}$ is the local unit normal vector to the surface pointing into the liquid, and v_n and κ denote the normal velocity and the curvature of the interface, respectively. Equation (11) is the Stefan condition, which relates the velocity of the interface to the difference in the heat currents between the solid and liquid side of the interface, and equation (12) is the generalized Gibbs-Thomson equation that gives the temperature at the interface as a function of the interface curvature and velocity. In this equation, d_0 is the capillary length defined above, and β is the linear kinetic coefficient (proportional to the inverse of the interface mobility). These macroscopic quantities are related to the parameters of the phase-field model by

$$d_0 = a_1 \frac{W}{\lambda}, \tag{13}$$

$$\beta = a_1 \left(\frac{\tau}{\lambda W} - a_2 \frac{W}{D} \right), \tag{14}$$

where a_1 and a_2 are constants of order unity that only depend on the choice of the various interpolation functions, and that are equal to $a_1 = 5\sqrt{2}/8$ and $a_2 = 0.6267$ for the choices made here [13]. These formulae can be used to fix the only undetermined parameter that is left in the model, the relaxation time τ of the phase field.

It is worth while to comment on the use of this phase-field model. The macroscopic model contains two interfacial parameters: the capillary length and the kinetic coefficient, which are fixed constants for a given material. Phase-field modelling can be performed with an arbitrary interface thickness W, provided that the parameters λ and τ are chosen according to equations (13) and (14), as long as the constraints for the validity of the asymptotic analysis are respected, that is, as long as the interface thickness is small enough. When the same simulation is repeated with different values of W, the results depend only quadratically on W, which means that a good approximation for the sharp-interface result can be obtained even with quite large interface thickness [13,14,15].

For the simulation of dendrites, interfacial anisotropy needs to be provided. Both the surface free energy and the interface mobility can depend on the orientation of the interface with respect to the crystallographic axes. These effects are incorporated by making W and τ depend on the local surface normal, as detailed in Ref. [13]. With the additional help of multi-scale algorithms for the resolution of the diffusion equation, it is then possible to simulate dendritic growth in three dimensions, both at low [20,21,22] and high [23] undercoolings. As an example, Fig. 1 shows a Nickel dendrite and the curve of growth velocity versus undercooling obtained from experiments and simulations. It should be mentioned that the kinetic parameters of the interface (absolute value and anisotropy of β) cannot be determined experimentally, and have been calculated by molecular dynamics simulations.

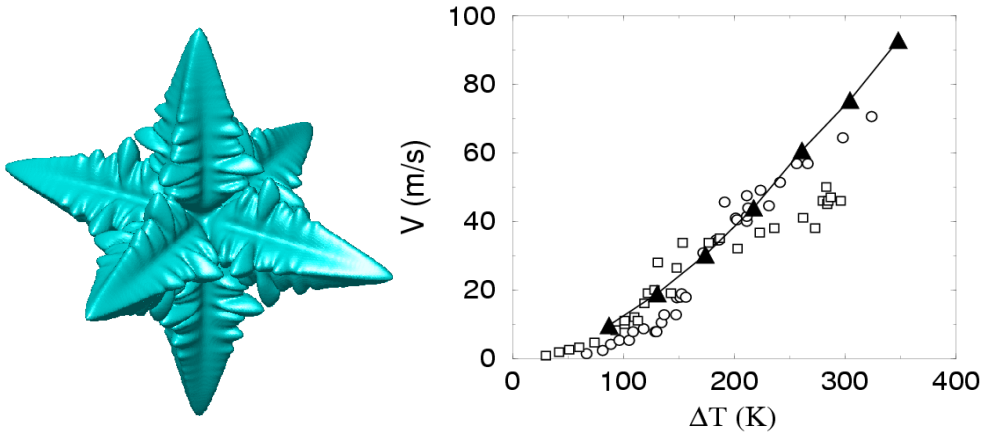

FIGURE 1. Left: snapshot picture of a growing Nickel dendrite simulated with the phase-field model. Right: growth speed of the tips as determined by simulations (full symbols) and experiments (open symbols). From Bragard *et al.* [23].

Phase-field modeling of solidification is of course not limited to pure substances. Various models for alloy solidification, including alloys with multiple phases and components, have been developed [14,15,24,25,26,27,28]. Not all of the models have the same degree of precision as the model outlined above. The key to a precise mapping between macroscopic and model parameters is the completion of the asymptotic analysis. One of the active areas of research in phase-field modeling is to extend this analysis to models with ever increasing complexity (for a concise recent review, see [29] and references therein), which sometimes leads to long analytic calculations. An important

remark is that, in view of the complexity of the models, an analytic calculation without numerical tests can miss some important effects. Therefore, if quantitative simulation results are desired, only those models should be used for which extensive benchmarking has been carried out, either by comparison of numerical results with some known analytic solutions, or by a convergence study of the model with decreasing interface thickness.

EPITAXIAL GROWTH

A second application of the phase-field method in crystal growth is the modeling of step-flow dynamics during the epitaxial growth of terraced (vicinal) surfaces from vapor or solution. Contrary to solid-liquid interfaces, which are atomically rough, with atoms or molecules frequently hopping from one phase to the other, such surfaces are atomically smooth and consist of large terraces where a filled close-packed crystal plane is in contact with the vacuum (or the solution). These terraces are separated by well-localized steps which have a height of once the unit cell of the crystal. The incorporation of new atoms occurs predominantly at the steps. On an atomistic scale, such surfaces are conveniently described by the classic 'terrace-step-kink' picture. On the continuum scale, the starting point is the Burton-Cabrera-Frank (BCF) model [30] which describes the steps as smooth lines. Crystal growth is decomposed into two stages: adsorption of atoms onto the crystal surface (they become 'adatoms'), followed by diffusion along the surface and the incorporation of adatoms at the steps. As a consequence, the step motion is determined by the dynamics of the adatom concentration. This picture is valid as long as the concentration of kinks at the step edges is sufficiently high, that is, the steps themselves are rough.

The BCF free boundary problem for molecular beam epitaxy (MBE) is very similar to the one for solidification given by equations (10)-(12) and reads

$$\partial_t u = D\nabla^2 u + F - \frac{u}{\tau_s}, \tag{15}$$

$$v_n = \hat{n}\cdot\left(D\nabla u\big|_+ - D\nabla u\big|_-\right), \tag{16}$$

$$u_{\text{int}} = d_0\kappa + \frac{v_n}{k}. \tag{17}$$

Here, $u = \Omega\left(c - c_{eq}^0\right)$ is a dimensionless adatom concentration field, where Ω is the surface occupied by one atom in the close-packed crystal plane, c is the adatom concentration and c_{eq} its equilibrium value on a terrace next to a straight step. Equation (15), valid on each terrace, describes adatom diffusion, the deposition of new adatoms with a homogeneous rate F from the vapor, and desorption of adatoms back into the vapor with a characteristic desorption time τ_s. Equation (16) is the Stefan condition for step flow, which states that the velocity of a step is proportional to the fluxes of adatoms that arrive from the lower (+) and upper (-) terrace; the unit normal vector points into the lower terrace. Finally, equation (17) is the boundary condition for the adatom concentrations at the interface. Here, $d_0 = \Omega^2 c_{eq}^0 \gamma / k_B T$ (with γ the step free energy and k_B Boltzmann's constant) is the capillary length, and κ is the step curvature; k is the kinetic rate constant associated with incorporation of adatoms. Note that, in this model, the adatom concentrations at the interface on the upper and lower terraces are identical. This corresponds to the so-called transparent step model, in which steps do not represent any barrier for adatom diffusion.

In view of these similarities, it is quite obvious how the phase-field model developed above can be adapted for this problem. Instead of an interface between two phases, steps between an arbitrary number of terraces must be followed. Therefore, the double-well potential must be replaced by a multi-well potential, where each minimum corresponds to a terrace. The phase field is then simply proportional to the surface height. A tilt of this multi-well potential as a function of the value of u then favors growth or dissolution in response to a local super- or undersaturation. The equations of a simple phase-field model that has these properties are given by [31]

$$\tau\partial_t\phi = W^2\nabla^2\phi + \sin(\pi\phi) + \lambda u\left(1+\cos(\pi\phi)\right), \tag{18}$$

$$\partial_t u = D\nabla^2 u + F - \frac{u}{\tau_s} + \frac{1}{2}\partial_t\phi, \tag{19}$$

which generates terraces for odd integer values of ϕ ($|\phi|$=1,3,5, …). The relation between the macroscopic parameters d_0 and k and the model parameters is given by the analog of equations (13) and (14), with different values for the constants a_1 and a_2 that can be found in Ref. [31].

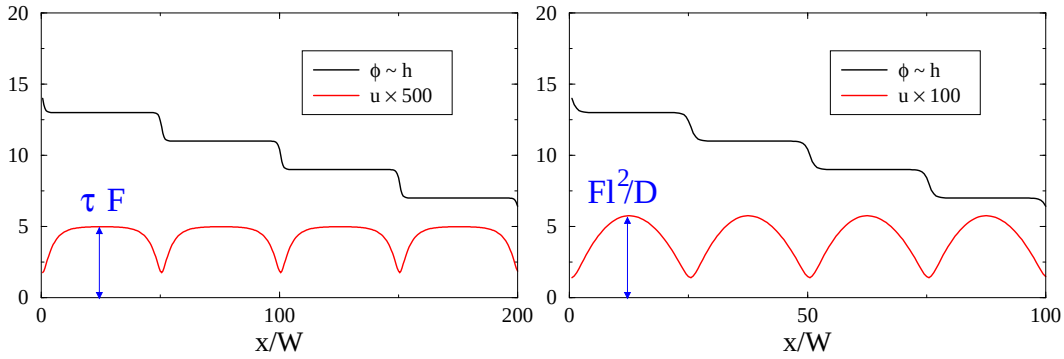

FIGURE 2. One-dimensional simulations of equations (18) and (19) corresponding to a linear step train. Left: the desorption length is smaller than the terrace size, the dynamics of steps is local. Right: the desorption length is larger than the terrace size, the dynamics of the steps is nonlocal since neighboring steps are coupled.

As an illustration for how this model can be used to understand the evolution of stepped surfaces, Figure 2 shows two examples of one-dimensional simulations of equations (18) and (19). A series of terraces is generated as an initial condition, and only a small part of the step train is shown. The behavior of the system depends on the ratio of the terrace size l and the characteristic desorption length $x_s = \sqrt{D\tau_s}$ (it should be noted that for well-converged simulations the interface thickness W must be much smaller than the desorption length). If the desorption length is smaller than the terrace size, the adatom concentration in the center of the terraces is determined by the equilibrium between the incoming flux and desorption. This means that the concentration gradients which drive the growth of a step are localized in the neighborhood of the step, such that there is no interaction between the steps (figure 2, left graph). In contrast, if the desorption length is larger than the terrace size, the gradients around one step are determined by the distance and shape of the next step (the maximum concentration in the center of the terrace is given by Fl^2/D), and the motion of neighboring steps gets strongly coupled (figure 2, right graph). It is in this latter regime that the phase-field approach is the most useful, since it makes it possible to simulate steps in arbitrary geometry. For instance, spiral surface growth has been investigated in Ref. [31].

Since its development, this model has been extended and applied to various situations, see Ref. [7] for examples. In particular, as already mentioned, the above model does not incorporate barriers at the steps (for instance, the Ehrlich-Schwoebel effect). A model that includes such barriers needs to allow for different adatom concentrations on the two sides of a step, which was achieved by a model that uses two separate concentration fields (one for each terrace) at each step [32].

CONCLUSIONS

The above examples show that the phase-field method is capable of simulating complex phenomena with simple equations. The models presented above are only some of the simplest possible examples for phase-field models and are therefore only a pedagogical starting point for a more detailed study of the subject. Many more examples can be found in recent reviews of the phase-field method [3-10]. The development of new and even more complex models is an active area of research. A major challenge is to develop models for complex growth processes, in which the dynamics of interfaces are driven by more than one physical phenomenon. Examples include the coupling of solidification, fluid flow, and elastic effects in the growth of materials, electromigration of voids and islands, electrochemical growth and the growth of multicomponent systems. The versatility and flexibility of the phase-field method will certainly lead to rapid progress on these and many other problems.

REFERENCES

1. J. S. Rowlinson, *J. Stat. Phys.* **20**, 197-244 (1979).
2. J. W. Gibbs, "On the equilibrium of heterogeneous substances," in *The collected works of J. W. Gibbs*, New York: Longmans, 1928, pp. 55-353.
3. D. M. Anderson, G. B. McFadden and A. A. Wheeler, *Annu. Rev. Fluid Mech.* **30**, 139-165 (1998).
4. W. J. Boettinger, J. A. Warren, C. Beckermann and A. Karma, *Annu. Rev. Mater. Res.* **32**, 163-194 (2002).
5. M. Plapp, *J. Cryst. Growth* **303**, 49-57 (2007).
6. I. Singer-Loginova and H. Singer, *Rep. Prog. Phys.* **71**, 106501 (2008).
7. H. Emmerich, *Adv. Phys.* **57**, 1-87 (2008).
8. I. Steinbach, *Model. Simul. Mater. Sci. Eng.* **17**, 073001 (2009).
9. L.-Q. Chen, *Annu. Rev. Mater. Res.* **32**, 113-140 (2002).
10. Y. Wang and J. Li, *Acta Mater.* **58**, 1212-1235 (2010).
11. A. Karma, "Phase field modeling", in Handbook of Materials Modeling, Vol. I, edited by S. Yip, Amsterdam: Springer, 2005, pp. 2087-2103.
12. Q. Bronchart, Y. Le Bouar and A. Finel, *Phys. Rev. Lett.* **100**, 015702 (2008).
13. A. Karma and W.-J. Rappel, *Phys. Rev. E* **57**, 4323-4349 (1998).
14. B. Echebarria, R. Folch, A. Karma and M. Plapp, *Phys. Rev. E* **70**, 061604 (2004).
15. R. Folch and M. Plapp, *Phys. Rev. E* **72**, 011602 (2005).
16. R Folch, J. Casademunt, A. Hernandez-Machado and L. Ramirez-Piscina, *Phys. Rev. E* **60**, 1724-1733 (1999).
17. R Folch, J. Casademunt, A. Hernandez-Machado and L. Ramirez-Piscina, *Phys. Rev. E* **60**, 1734-1740 (1999).
18. S.-C. Huang and M. Glicksman, *Acta Metall.* **29**, 701 (1981).
19. U. Bisang and J. H. Bilgram, *Phys. Rev. Lett.* **75**, 3898-3901 (1995).
20. N. Provatas, N. Goldenfeld and J. Dantzig, *J. Comput. Phys.* **148**, 265-290 (1999).
21. M. Plapp and A. Karma, *J. Comput. Phys.* **165**, 592-619 (2000).
22. A. Karma, Y. H. Lee and M. Plapp, *Phys. Rev. E* **61**, 3996-4006 (2000).
23. J. Bragard, A. Karma, Y. H. Lee and M. Plapp, *Interface Science* **10**, 121-136 (2002).
24. A. A. Wheeler, W. J. Boettinger and G. B. McFadden, *Phys. Rev. A* **47**, 1893 (1993).
25. J. Tiaden, B. Nestler, H.-J. Diepers and I. Steinbach, *Physica D* **115**, 73 (1998).
26. S. G. Kim, W. T. Kim and T. Suzuki, *Phys. Rev. E* **60**, 7186 (1999).
27. J. C. Ramirez, C. Beckermann, A. Karma, H.-J. Diepers, *Phys. Rev. E* **69**, 051607 (2004).
28. J. Eiken, B. Böttger and I. Steinbach, *Phys. Rev. E* **73**, 066122 (2006).
29. M. Plapp, Phil. Mag., in press (2010); arXiv:1004.4502 (2010).
30. W. K. Burton, N. Cabrera and F. C. Frank, *Philos. Trans. R. Soc. London A* **243**, 299 (1951).
31. A. Karma and M. Plapp, *Phys. Rev. Lett.* **81**, 4444-4447 (1998).
32. O. Pierre-Louis, *Phys. Rev. E* **68**, 021604 (2003).